Analytical Methods

Accepted Manuscript

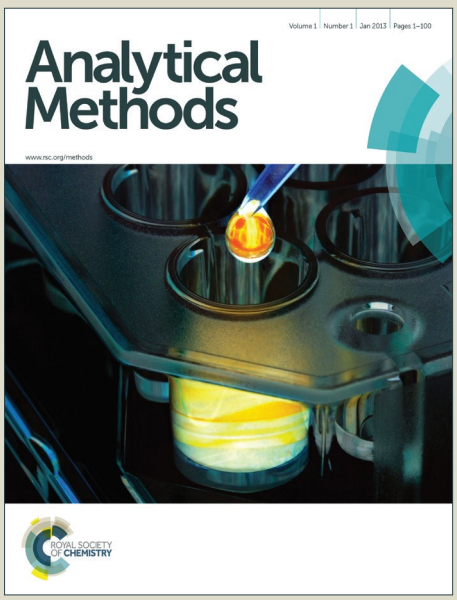

This is an *Accepted Manuscript*, which has been through the Royal Society of Chemistry peer review process and has been accepted for publication.

Accepted Manuscripts are published online shortly after acceptance, before technical editing, formatting and proof reading. Using this free service, authors can make their results available to the community, in citable form, before we publish the edited article. We will replace this *Accepted Manuscript* with the edited and formatted *Advance Article* as soon as it is available.

You can find more information about *Accepted Manuscripts* in the Information for Authors.

Please note that technical editing may introduce minor changes to the text and/or graphics, which may alter content. The journal's standard Terms & Conditions and the Ethical guidelines still apply. In no event shall the Royal Society of Chemistry be held responsible for any errors or omissions in this *Accepted Manuscript* or any consequences arising from the use of any information it contains.

ROYAL SOCIETY OF CHEMISTRY

www.rsc.org/methods

An experimental study on the evolution of aggregate structure in coals of different ranks by in-situ X-ray diffractometry

Wenyong Zhang*[,a], Shancheng Chen[a], Feng Han[a], DunWu[a]

[a] *Exploration Research Institute, Anhui Provincial Bureau of Coal Geology, Hefei, Anhui 230088, China*

Abstract

Coal samples of different ranks were selected based on geological ages and regions to investigate their thermal evolution in aggregated structure by *in-situ* X-ray diffraction spectroscopy (XRD). Samples were heated under at a rate of 10 °C/min in the range of 25 to 900 °C. The results show that the XRD profiles of the coals displayed an evident peak weakness at 20° (λ-band), suggesting the decomposition of oxygen-containing functional groups in coal matrix at higher temperature. By contrast, the peak at 26° (so-called *G*-band) became sharper and shifted to higher angles, reflecting a more ordered crystallite structure of coal with increasing heating temperature. It is noted that the integrally diffracted intensity of these two bands weakened intensely above 400 °C, suggesting that the coal aggregate structure may be loosen due to depolymerization of the carbonaceous matrix in coal. The primary phase of weight loss for the low-rank coals took place in 300-500 °C, but the high-rank coals had obviously second pyrolysis reaction above 500 °C. Moreover, this study shows that the heating temperature effect played a key role in the evolution of the interlayer spacing of the crystalline structure (d_{002}) and the height of aromatic layers (L_c), while the diameter of aromatic layers (L_a) was more dependent on coal ranks rather than heating temperature.

Keywords: In-situ; *X-ray diffraction*; aggregate structure; coal

* Corresponding author: Tel: +86-551-65846042; fax: +86-551-65846042.

E-mail address: adam854621@163.com (Zhang Wenyong)

1. Introduction

Coal resource is and will continue to be the primary energy source for power generation in China. However, the large volumes of coal used in the energy and industrial sectors have made coal combustion the dominant greenhouse gases emission source.[1-2] Hence, in order to rapidly improve environment pollution from mining, the Chinese government put forward the cleaning utilization of coal all over the country. However, there is an increasing demand for coals, especially, because of the fact that crude petroleum reserves are obviously declining. It has long been supposed that the aggregate structure of coal play an important role in the cleaning utilization of coal.[3] Nearly all conversion technologies of coal require the thermal treatment but pyrolysis is the initial phase in the most coal conversion processes. What is more, the physicochemical properties of coal are of vital importance on the efficiency of coal conversion.[4-9] Two competitive processes happen when coal is heat-treated. One is the depolymerization by which the gaseous (e.g. gas and water vapor) and liquid products (e.g. tar) are generated. Another is the polycondensation leading to appearance of the turbostratic lamellar system. Amounts of heterogeneous pyrolytic reactions take place in these two types of competitive processes.[10] In addition, a better knowledge of the thermal behavior of coals with different metamorphism is necessary in order to assess their potential for being used in

certain coal utilization processes. Therefore, to explore deeply coal processing and utilization, the study on the structural characteristics of coal under heat-treated condition is necessary since it can provide new insights into the evolution of coal composition and physicochemical structure.

Coal is a heterogeneous sedimentary rock, primarily consisting of molecules with polyaromatic and polynuclear structures and associated heteroatom groups.[11] Despite such importance of coal aggregate structure, its direct detection method has not been realized entirely. Currently, analytical techniques such as nuclear magnetic resonance (^{1}H and ^{13}C NMR), Fourier transform infrared spectroscopy (FTIR), and X-ray diffraction (XRD) are widely used for determining the physicochemical structures of macromolecules in coal.[12-14] Compared with the NMR and FTIR, XRD has the advantage of simplicity and affordable technique for better understanding of ordered packing of.[15] In the past couple of decades, teams of researchers have proposed several structural parameters for evaluating the molecular structure of coal and other less-crystalline carbonaceous materials through the use of XRD. For example, the XRD profiles of carbonaceous materials with low-crystallinity has been statistically interpreted by Hirsch[16] and Diamond[17]; Fujimoto and Shiraishi[18] modified the Diamond's method for estimating carbon-layer sizes and; Takagi[19] and Mennelia[20] used a standard analysis of carbon stacking structure to understand the stacking structure of coal and other less-crystalline carbonaceous materials. Lu et al.[21] had conducted a systematic study on the evolution of L_a of different types of coal, proving that the development of L_a was more dependent on coal rank. Nevertheless, the reports about the evolution characteristics of coal aggregate structure during the heat treatment were relative lack. Only Li et al.[22] definitely proposed the increase tendency on L_a with the increase of temperature by *in-situ* XRD. Thus, a clear and unambiguous knowledge on the changes of the crystallite parameters of coal with different ranks under heat treatment is still the urgent problem.

Owing to the complication of the reaction process of coal during the heat treatment, the *ex*-line analysis methods could not reveal the real pyrolysis process. Thus, in the present study, the *in-situ* XRD analytical techniques, taken at real temperature without cooling the coal samples, were used to investigate the effect of heating temperature on the coal aggregate structure in detail. In addition, there were relationship between elemental composition of coal and coal aggregate structure.

2. Samples and experiment

2.1 Samples preparation

Four Chinese coal samples with different ranks were choose in the present study (mine, origin, age and sample rank shown in Table 1). These Permo-Carboniferous coal samples (HN, KL and SY) formed from continental deposit belong to the North China coal-accumulating basin. The Permian coal sample (ZJ) formed from marine deposit belongs to the Yangtze platform. These samples were derived from different metamorphic types, leading to the differences in coal rank. The bulk samples were ground to 200 mesh, and kept under an inert N_2 atmosphere before analysis. The raw samples were demineralized before XRD experiment by means of HF+HCl+$HClO_4$ with the purpose of avoiding the interference of mineral matters. A detailed demineralized procedure of raw coal can be found in Wu et al.[23] Proximate analyses of these samples were carried out according to ASTM Standards D3173-03, 2005 (M_{ad}),[24] D3174-04,

2005 (A_{ad}),[25] D3175-02, 2005 (V_{ad}),[26] respectively. Ultimate analyses were performed by GB/T 476-2008,[27] GB/T 214-2007,[28] and GB/T 215-2003,[29] severally. These results are listed in Table 2.

2.2 Wight loss measurement

The configurations of the STA 409C Thermo-Gravimetric Analysis (TGA) apparatus were detailed elsewhere.[30] Approximately 20 mg of each demineralized coal sample was placed in a platinum crucible and heated from room temperature to 750 °C at a heating rate of 10 °C/min, using N_2 as the carrier gas at a constant flow rate of 50 mL/min. The weight loss of the coals during the heat treatment was recorded continuously as a function of temperature, from which the curves of TG and DTG were also obtained.

2.3 In-situ X-ray diffraction

In order to obtain noteworthy results, the experiments were performed via carefully selected coal samples. The *in-situ* XRD data collection was carried out on Philips X'Pert PRO X-ray powder diffraction, using crystal-reflected and Ni-filtered Cu Kα radiation, and a scintillation detector. The XRD pattern was recorded over a 2θ interval of 10-60°, with a step size of 0.034° and 2 s/step counter time. Powered coal samples were heated from room temperature to 900 °C with the heating rate of 10 °C/min. The above mentioned coal samples were kept at individual target temperature points for 20 min to be detected by XRD equipment. The *in-situ* profiles were measured at each temperature.

The structural parameters of coal including the lateral size (L_a) and the stacking height (L_c) were determined using the conventional Scherrer equations:

$L_a=1.84\lambda/B_a\cos(\varphi_a)$ (1)

$L_c=0.89\lambda/B_c\cos(\varphi_c)$ (2)

Where λ is the wavelength of the radiation used, B_a and B_c are full width at half maximum of (d_{100}) and (d_{002}) peaks, φ_a and φ_c are the corresponding scattering angles or peak positions.

To obtain further data, peak separation and semi-quantitative calculation of XRD diffractograms were performed by the curve-fitting program of Origin software. The broad peak around 25° in the XRD diffractograms was deconvoluted into two Gaussian peaks: λ-band (20°) and *G*-band (26°). The detailed processes for curve-fitting were described in Wu et al.[23]

3. Results and discussion

3.1 Relationship between elemental composition and coal aggregate structure

Aggregate structure of coal can be estimated from its elemental compositions.[15] Table 2 shows that the atomic H/C ratio in coal decreases with the increase of coal ranks, suggesting that the chemical structure of coal is closely associated with the its elemental compositions. As suggested by Hirsch,[15] there is a corresponding relationship between C_{daf} content in coal and coal aggregate structure (Fig. 1). Lignite and subbituminous coals, i.e. SY and KL, with <85% C_{daf} have an "open" structure with lamellae rarely orientated and connected by cross-links, while bituminous coals, i.e. HN, with C_{daf} between 85% and 91% has a "liquid" structure with lamellae partly orientated and abundant cross-links interrupted. For the coal (ZJ) with >91% C_{daf} has an "anthracitic" structure with both lamellae and pores orientated.

3.2 Change in XRD profiles of coals by heat treatment

Using the van Krevelen and Schuyer method,[31] we obtain first a strong diffused diffraction

line, which amounts to d_{002} of graphite. Fig.2 shows the XRD profiles of KL (subbituminous) and SY (lignite) coals before and after the heating treatment. The raw SY coal exhibited abroad peak at $2\times sin\theta/\lambda$=0.24 ($\lambda$-band) with a broad shoulder at $2\times sin\theta/\lambda$=0.28 (*G*-band). In the temperature range of 100-400 °C, the SY coal heat-treated showed the more intensified λ-band in comparison with that of non-treated coal. By contrast, relative intensities at *G*-band were attenuated after the coal was heated. In addition, a slight increase of d_{002} value (calculated by Scherrer equations) was observed from 0.3567 nm (raw coal) to 0.3585 nm (400 °C) (Table 3). When temperature was above 400 °C, the coal heat-treated exhibited intensified diffraction at *G*-band along with the decreased diffraction at λ-band (Fig. 2 (inset), at temperature range of 600-900 °C), and the shape of *G*-band band became sharper and shifted to higher angles. However, it is noted that the integrally diffracted intensities of these two bands in the XRD profiles weakened above 400 °C, suggesting that the aggregate structure of coal may be loosen by the depolymerization of the carbonaceous matrix in coal.[22] The similar tendency was observed in KL coal, although the change in its XRD profiles occurred at a lower temperature of 25 °C. This indicates that KL coal had higher total contents of carboxylic groups than those in SY coal.[22] It was further observed that the (*100*) band, attributed to the extension of aromatic molecules in the plane structure of the crystallites, became narrower with increasing temperatures.

Fig. 3 illustrates the XRD profiles of HN and ZJ of higher rank coals before and after the heating treatment. The heating of ZJ coal at >400 °C sharpened the peak at *G*-band whilst with a small extent compared to those of the non-treated one, due to the thermoplasticity of the "anthracitic" structure. Based on Scherrer equations, the d_{002} value of ZJ coal slightly decreased from 0.3496 nm to 0.3485 nm when the coal was heated from 25 to 400 °C, and then declined continuously above 400 °C (Table 3). On the contrary, the d_{002} value of HN coal increased from 25 to 400 °C, and then decreased above 400 °C.

3.3 Structural change of coals by the heat treatment

Table 4 lists the thermal parameters of the coals. Fig. 4(a) shows the relative mass and weight loss rate of ZJ coal during the heat treatment for illustration. The relative mass of ZJ coal only changed ~3% from 100 to 300 °C. Degassing reactions usually take place in this temperature range, which could lead to the thermal decomposition of the labile structure of coal matrix, accompanying by the release of light gaseous species (H_2O, CH_4, CO_2, and N_2). The relative mass variation due to H_2O and CO_2 loss was more significant in the lower rank coals of KL and SY because of their higher oxygen contents (Table 2 and Table 4).[22] This indicates that the contribution to structural change for some condensation reactions derived through the degassing action was negligible compared to the liberation of hydrogen bonds[32] during the heat treatment <300 °C. The relative mass of ZJ coal decreased significantly with the temperature until ~500-600 °C, indicating that the thermal cracking of covalent bonds such as methylene and ether linkages may take place at ~500 °C. At 600 °C, the relative mass loss of ZJ coal reached approximately 57.5% with a maximum weight loss rate of -0.71 %/°C. Due to the differentiation of coal aggregate structure (Fig. 1), the relative mass loss of KL and SY was more evident between 300 °C and 500 °C, suggesting that gas formation as well as coking reactions may initiate ~300 °C in low-rank coals.

The weight loss rate curves of all coals during the heat treatment were shown in Fig. 4(b) for

comparison. With the increase of coal ranks, the temperatures of maximum rate of weight loss increased accordingly from 454.1 to 599.8 °C. The rates of weight loss of ZJ and KL coals are greater than those of HN and SY coals, suggesting that pyrolytic reactions took place more frequent in the former coals.[22, 32] Additionally, due to the low-rank coals with more side chains and activating groups which leads to their molecular structure more readily decomposed at <550 °C in comparison to the high-rank coals, the primary phase of weight loss for the low-rank coals takes place in 300-500 °C, but the high-rank coals have obviously second pyrolysis reaction above 500 °C (Table 4).

3.4 The structural characterization of the coals during the heat treatment

For the detailed analysis of the XRD data, the diffraction curves were evaluated by a fitting procedure in Wu et al.[23] Computation and fitting were performed in the 2θ range of 14-32° using the Origin 8.0 software. Fig. 5 illustrates the curve fitting procedures of XRD profiles of KL coal in 2θ range of 14-32° at 300 °C, 600 °C, and 900 °C, respectively. Fig. 6 shows the variation curves of crystallite parameters of the coals with increasing heating temperatures. As seen from Fig. 6(a), with the increase of heating treatment temperatures, the evolution trend of the interlayer spacing of the crystalline structure (d_{002}) could be partitioned into two evident stages. The first stage was in the range of 25-500 °C, where the d_{002} values increased remarkably. The second stage was in the range of 500-900 °C, where the d_{002} values decreased considerably. This result indicates that the d_{002} values could be controlled by the temperatures of heated coals. Table 3 also shows that with increasing the degree of coal metamorphism, the d_{002} values accordingly decreases. The results indicate that the change of d_{002} is controlled by the combination effect of coal ranks and heating temperatures. As seen from Fig. 6(b), the height of aromatic layers (L_c) increased progressively with the increase of temperatures. The paroxysmal increase in L_c at 500 °C may be connected with the structural change caused by the expulsion of free hydrocarbons (mainly methane and ethane) and others gases such as CO physically trapped in the coal. The former thermo-gravimetric experiments also consolidate this speculation. The removal of the amorphous carbons in the range of 25-500 °C left the remaining aromatic nuclei in a highly reactive state and no longer insulated from one another. The stacking height of aromatic layers becomes even much larger at >500 °C,[21] suggesting the increases of crystallite structure order of coal. This is consistent with Wang et al.[33] As shown from Fig.6(c), the diameter of aromatic layers (L_a) almost remained unchanged with the increase of heating temperatures, whereas it increases slightly with the increase of coal ranks (Table 3), indicating that the change in the diameter of aromatic layers may mainly depend on coal ranks rather than heating temperatures. Up to now, due to the complexity and heterogeneity of the average lateral sizes for aromatic layers, there are no definite conclusions about the effect of temperature on the evolution trend of L_a. Based on the experimental results, the emergence of constant diameter (around 2.98 nm) may be due to the constraints imposed by side chains,[21,22,32,33] which could prevent the adjacent crystallites from merging together during the heat treatment (Lu et al.[20]). Because of the interaction between pressure and geothermal gradient from coal basin, L_a increased gradually during coalification, implying that the development of L_a would not be direction-dependent.

4. Conclusions

In-situ XRD can provide the aggregate structure features of the coals. The deconvolution of

overlapping bands in XRD profiles by curve-fitting methods can obtain detailed crystallite parameters of coal. Some conclusions could be drawn in present studies: (1) The higher the coal rank is, the lower the atomic H/C ratio is, indicating that the differences of elemental composition in coal decide the type of coal structures mainly including "open" structure, "liquid" structure, and "anthracitic" structure. (2) With increasing heat treatment temperatures, the change in intensity of the λ-band and G-band shows that the crystallite structure order of coal increases gradually. (3) The primary phase of weight loss for the low-rank coals takes place in 300-500 °C, but the high-rank coals have obviously second pyrolysis reaction above 500 °C. (4) It is noted that the integrally diffracted intensity of the two bands in the XRD profiles weakened intensely above 400 °C, suggesting that the coal aggregate structure is likely loosen by the depolymerization of the carbonaceous matrix in coal. (5) The effect of heating temperatures on the evolution trend of d_{002} and L_c parameters should be primary, but the change in L_a may be decided by coal rank rather than temperature.

6. References

[1] O. O. Sonibare, T. Haeger and S. F. Foley, Energy, 2010, 35, 5347-5353.
[2] J. H. Wang, J. Du, L. P. Chang and K. C. Xie, Fuel Process. Technol., 2010, 91, 430-433.
[3] B. Feng, S. K. Bhatia and J. C. Barry, Carbon, 2001, 40, 481-496.
[4] R. W Bryers, Fuel Process. Technol., 1995, 44, 25-34.
[5] K. Matsuoka, H. Akiho, W. C. Xu, R. Gupta, T. F. Wall and A. Tomita, Fuel, 2005, 84, 63-69.
[6] S. Hanson, J. W. Patrick and A. Walker, Fuel, 2002, 81, 531-537.
[7] S. Niksa, Energy Fuels, 1996, 10, 173-187.
[8] T. K. Das, Fuel, 2001, 80, 489-500.
[9] C. D. Sheng, Fuel, 2007, 86, 2316-2324.
[10] M. N. Siddiqui, M. F. Ali, and J. Shirokoff, Fuel, 2002, 81, 51-58.
[11] E. L. Evans, J. L. Jenkins and J. M. Thomas, Carbon, 1972, 10, 637-644.
[12] A. Sharma, T. Kyotani and A. Tomita, Fuel, 2001, 80, 1467-1473.
[13] W. Wanzl, Fuel Process. Technol., 1988, 20, 317-336.
[14] V. I. José, M. Edgar and M. Rafael, Org Geochem., 1996, 24, 725-735.
[15] S. P. Yao, K. Zhang, K. Jiao and W. X. Hu, Energy Explor Exploit., 2011, 29, 1-19.
[16] P. B. Hirsch, Proc Roy Soc. London A, 1954, 226, 143-159.
[17] R. Diamond, Acta Crystallogr, 1958, 11, 128-138.
[18] H. Fujimoto and M. Shiraishi, Carbon, 2001, 39, 1753-1813.
[19] H. Takagi, T. Isoda, K. Kusakabe and S. Morooka, Fuel, 2004, 3, 2427-2433.
[20] V. Mennelia, G. Monaco, I. Colangeli and E. Bussoletti, Carbon, 1995, 33, 115-136.
[21] L. Lu, V. Sahajwalla, C. Kong and D. Harris, Carbon, 2001, 39, 1821-1854.
[22] M. F. Li, F. G. Zeng, H. Z. Chang, B. S. Xu and W. Wang, Int. J. Coal Geol., 2013, 116, 262-269.
[23] D. Wu, G. J. Liu, R. Y. Sun and X. F, Energy Fuels, 2013, 27, 5823-5830.
[24] ASTM D3173-03, Annual Book of ASTM Standards. Gaseous Fuels: Coal and Coke, vol. 05. 06. Test Method for Moisture in the Analysis Sample of Coal and Coke, 2005.
[25] ASTM D3174-04, Annual Book of ASTM Standards. Gaseous Fuels: Coal and Coke, vol. 05. 06. Test Method for Ash in the Analysis Sample of Coal and Coke, 2005.

[26] ASTM D3175-02, Annual Book of ASTM Standards. Gaseous Fuels: Coal and Coke, vol. 05. 06. Test Method for Volatile Matter in the Analysis Sample of Coal and Coke, 2005.
[27] GB/T 476-2008, Standards Press of China, Beijing, 2008. Pp. 1-16, (in Chinese).
[28] GB/T 214-2007, Standards Press of China, Beijing, 2007. Pp. 1-10, (in Chinese).
[29] GB/T 215-2003, Standards Press of China, Beijing, 2003. Pp. 1-8, (in Chinese).
[30] D. Wu, G. J. Liu, R. Y. Sun and S. C. Chen, Fuel, 2014, 119, 191-201.
[31] D. W. van Krevelen and J. Schuyer, Elsevier, Amsterdam, 1957, 352.
[32] A. Arenillas, F. Rubiera, J. J. Pis, M. J. Cuesta and M. J. Iglesias. J. Anal. Appl. Pyrol., 2011, 58, 685-701.
[33] S. Q. Wang, Y. G. Tang, H. H. Schobert, G. D. Mitchell, F. R. Liao and Z. Z. Liu, Int. J. Coal Geol., 2010, 81, 37-44.

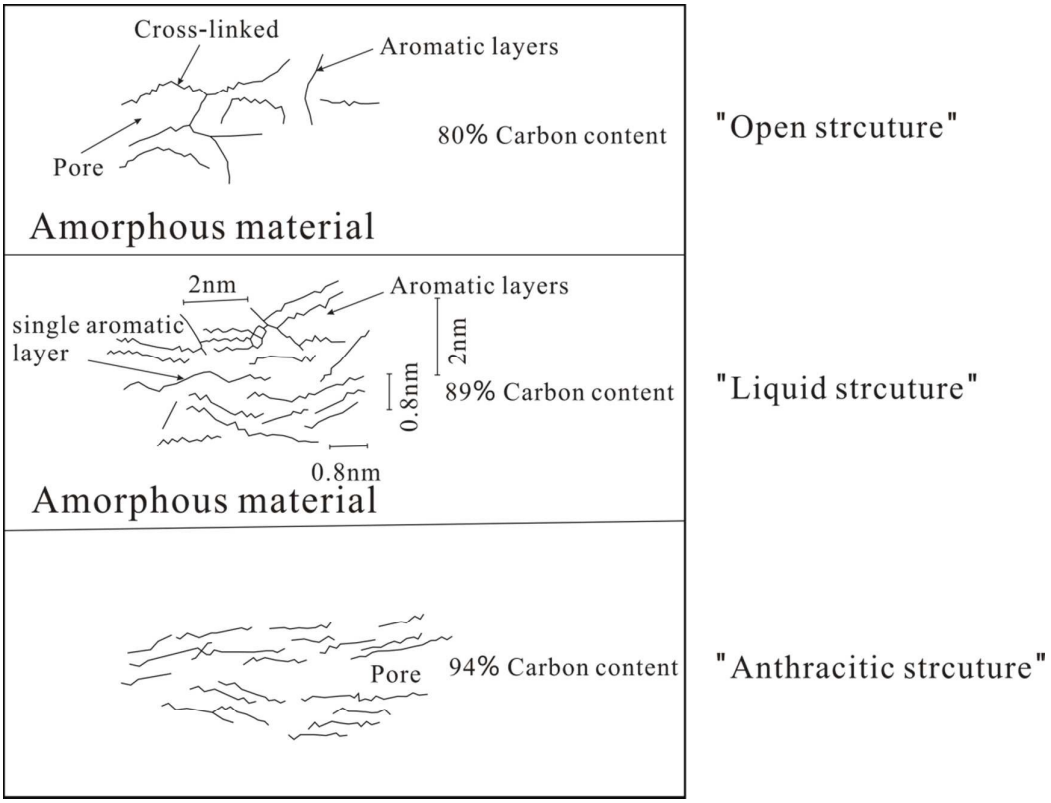

Fig. 1 The evolution of coal structure during coalification (modified by Hirsch [16]).

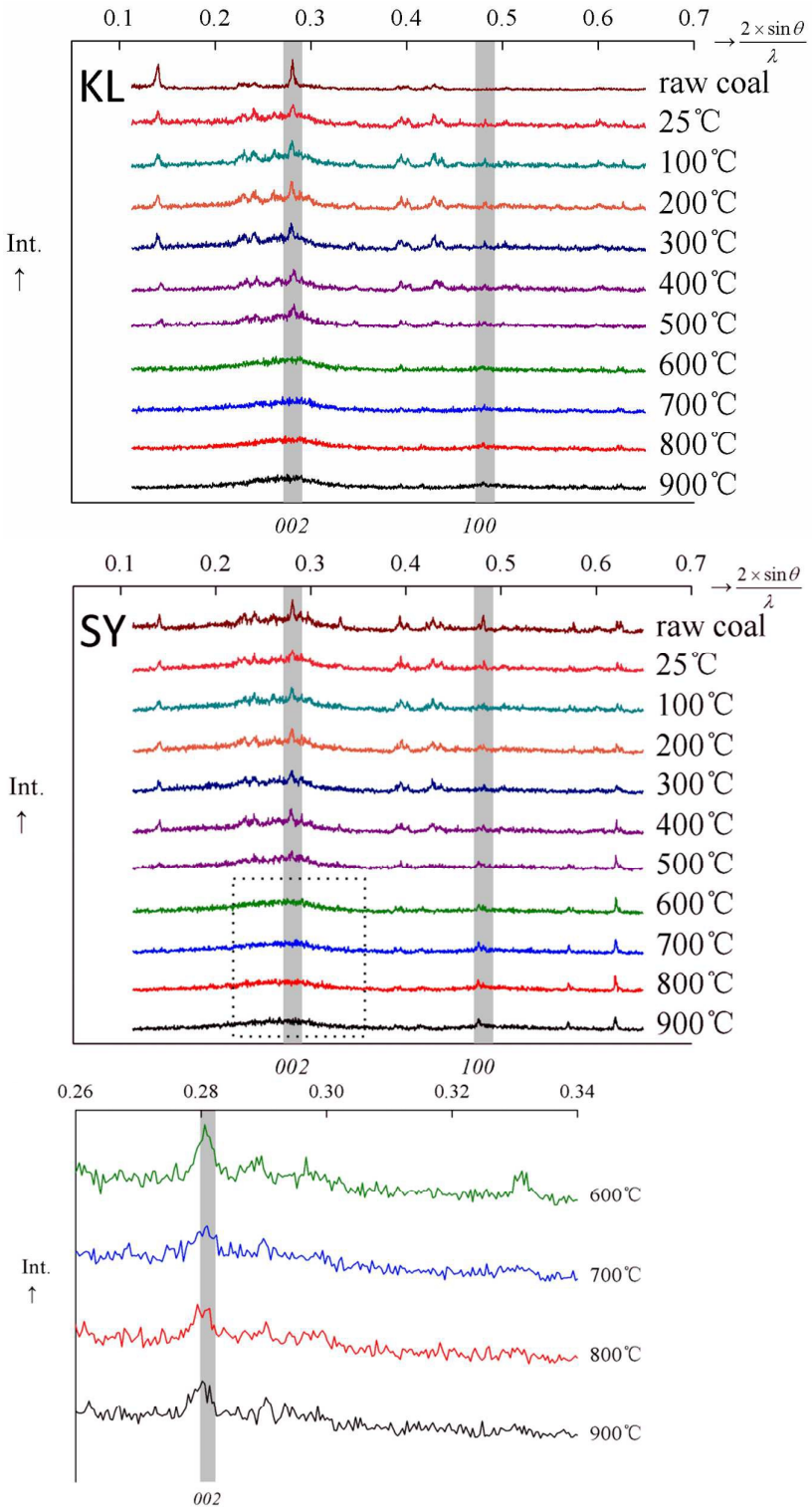

Fig. 2 XRD profiles of low-rank coals before and after the heating treatment.

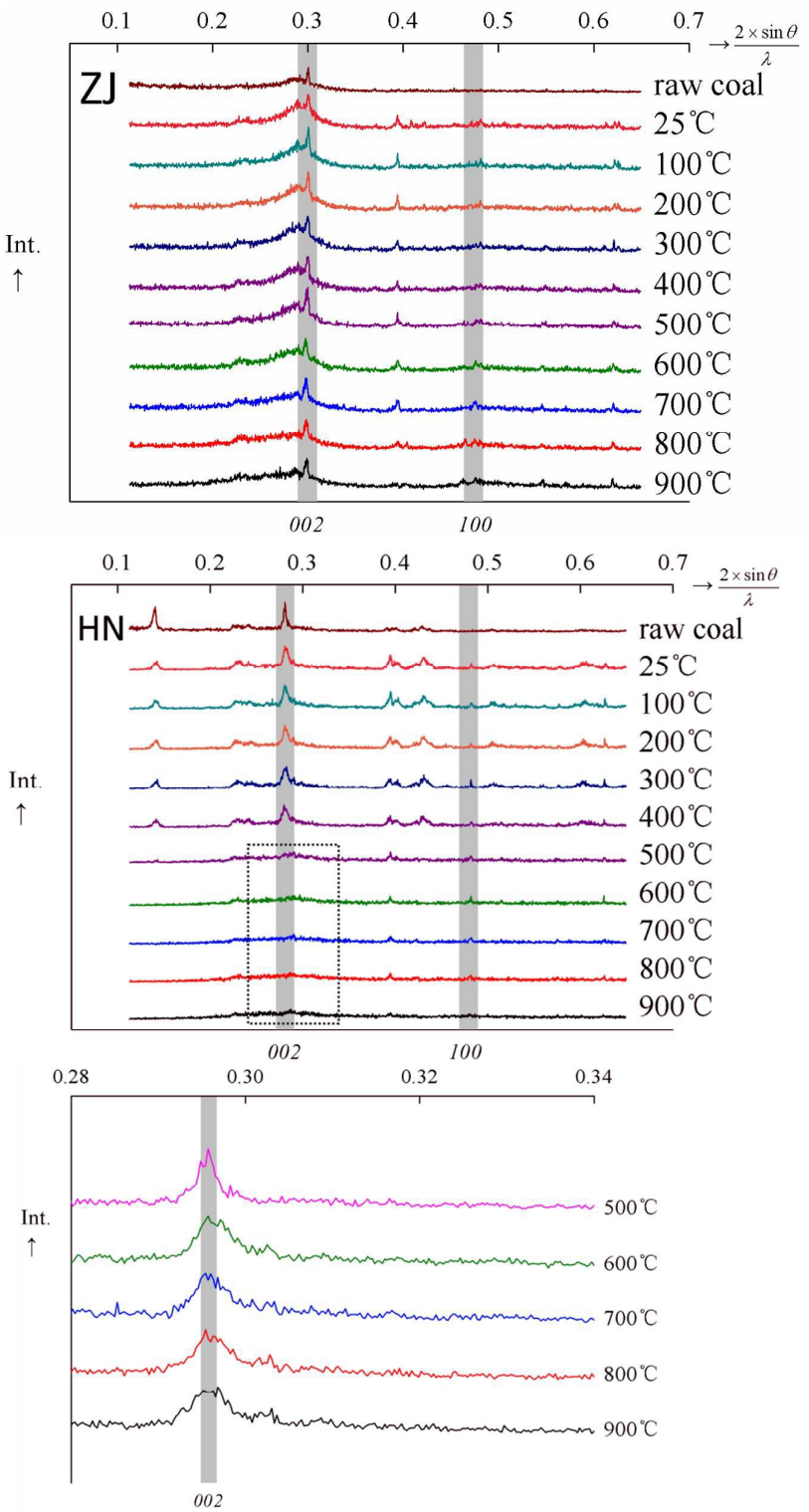

Fig. 3 XRD profiles of high-rank coals before and after the heating treatment.

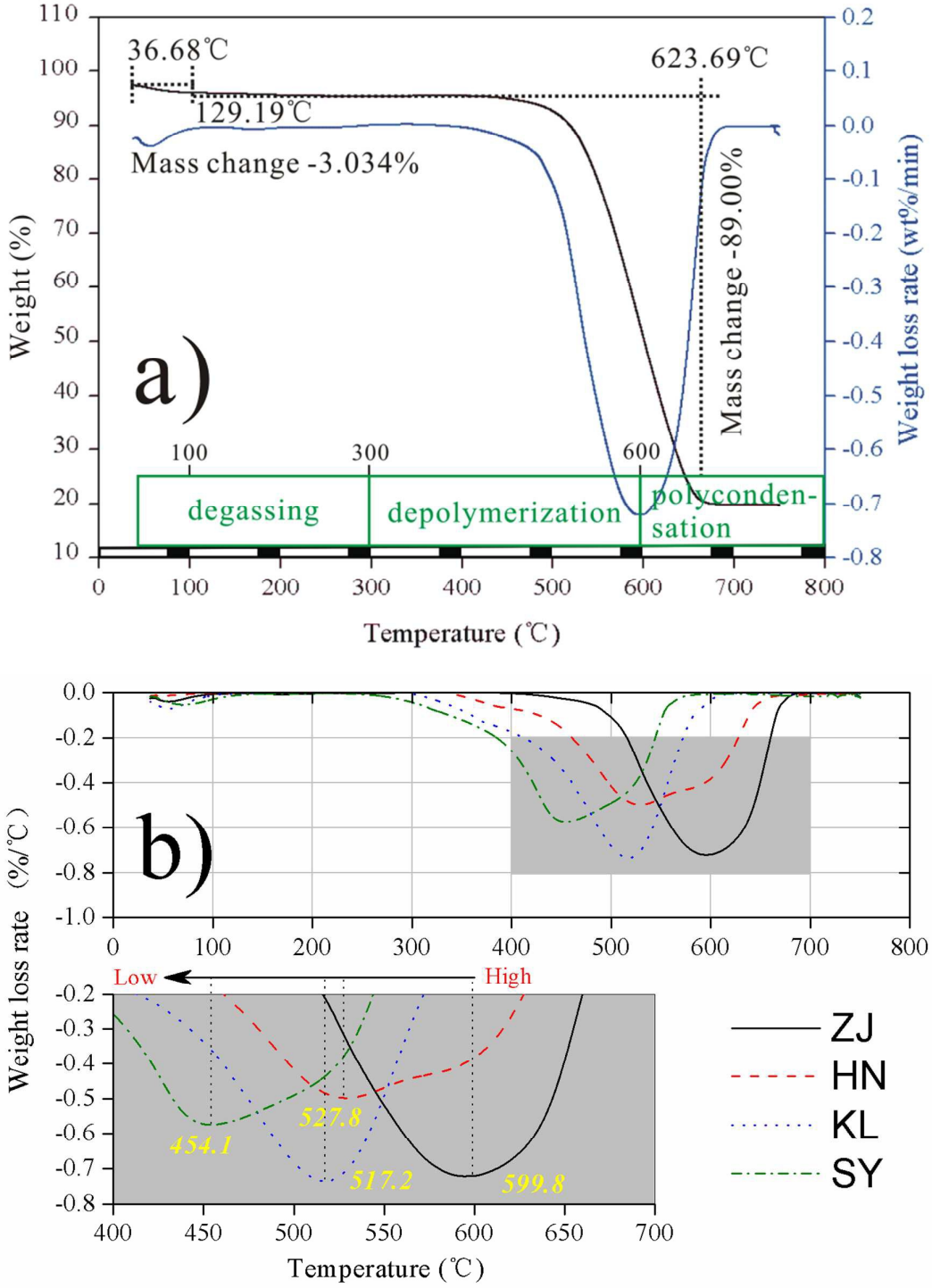

Fig. 4 (a) Weight and weight loss rate curves of ZJ coal (10 °C/min). (b) Variation of the rate of mass loss of the coals.

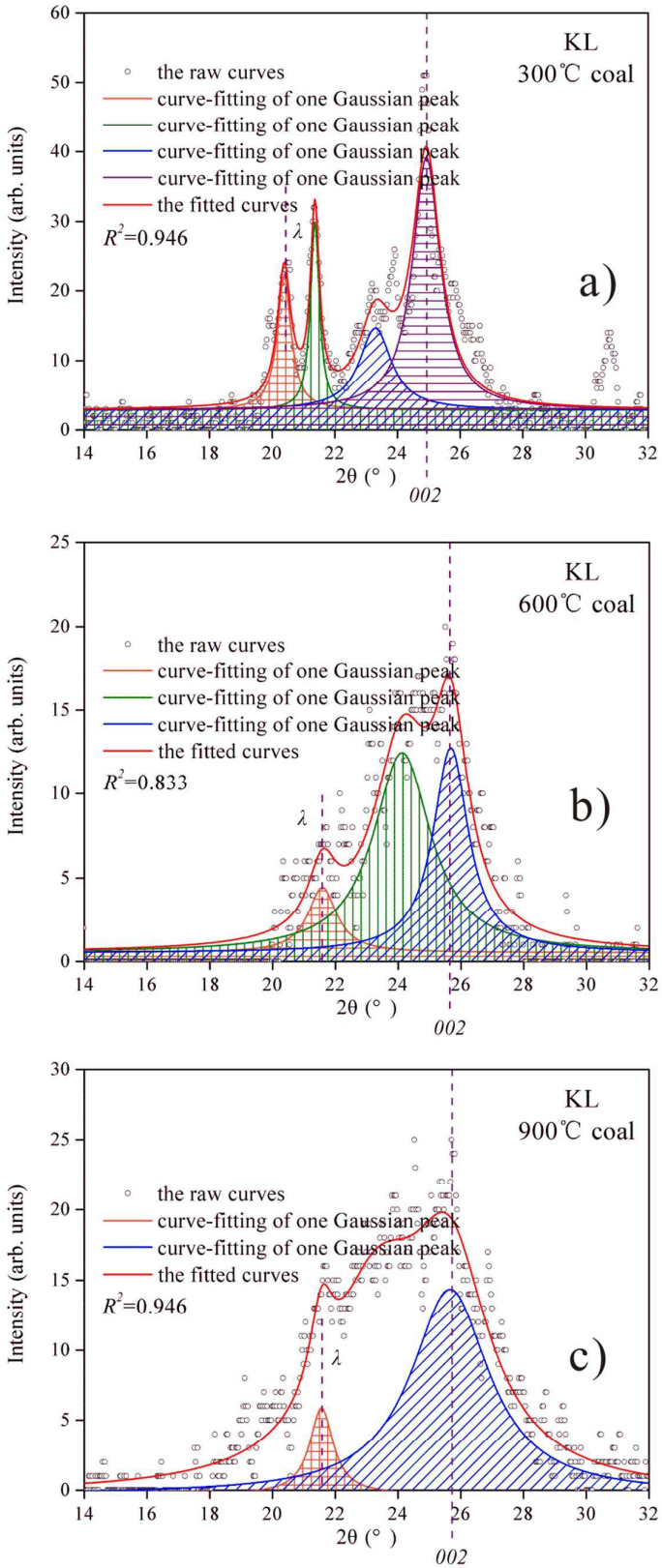

Fig. 5 Curve-fitting of XRD profiles of heat-treated KL coal in *2θ* range of 14-32° at (a) 300°C, (b) 600°C, and (c) 900 °C, respectively.

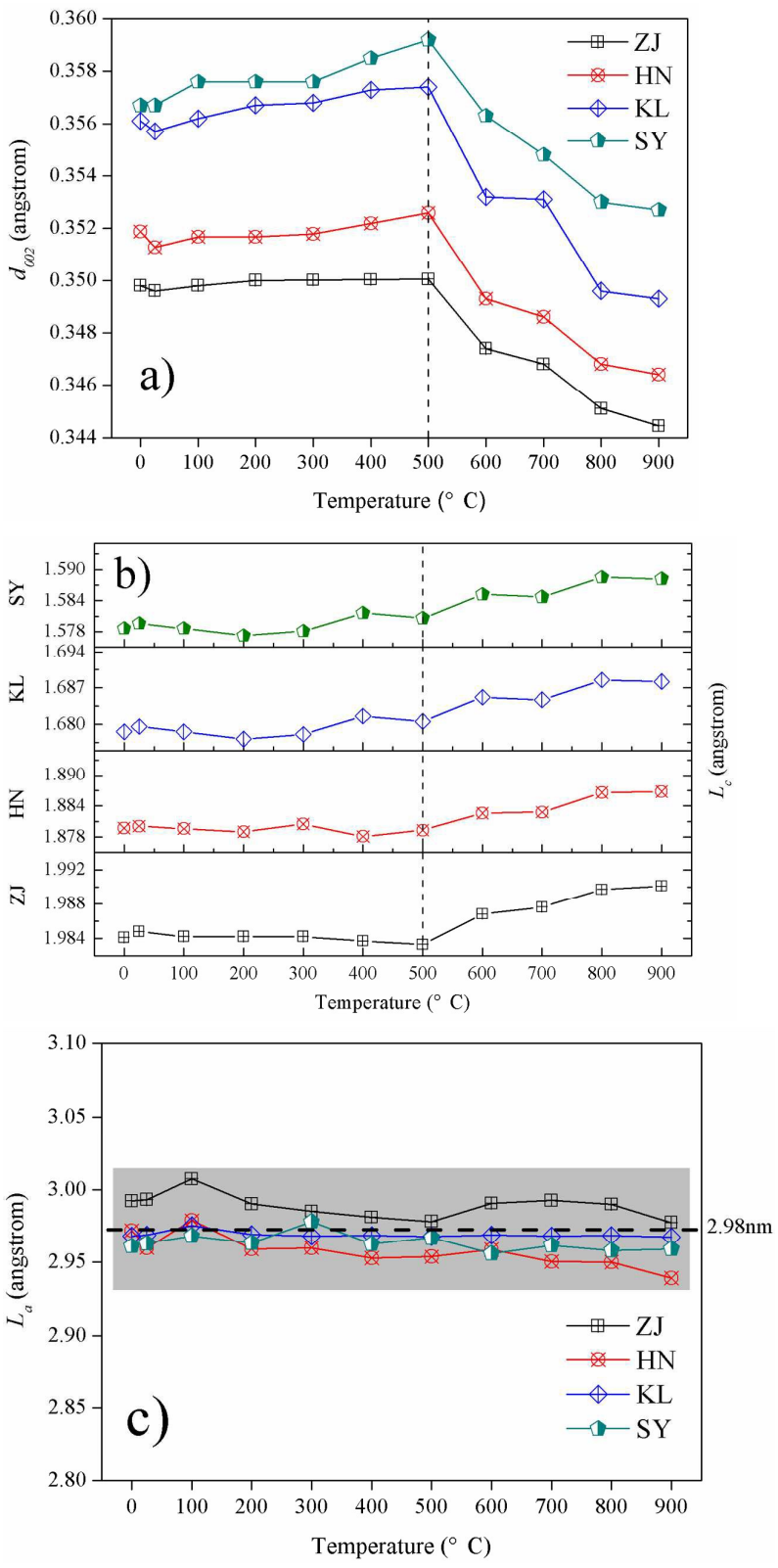

Fig. 6 Effect of heating treatment on the crystallite parameters of the studied coals.

Table 1 Mine, origin, age, and rank of coal samples

ID	Mine	Origin	Age	Rank	
ZJ	Zhijin	Guizhou	Late Permian	Anthracite	High-rank coals
HN	Huainan	Anhui	Late Permian	High volatile C	
KL	Kailuan	Hebei	Early Permian	Subbituminous	Low-rank coals
SY	Shanyin	Shanxi	Late Carboniferous	Lignite	

Table 2 Proximate and ultimate analyses of coal samples

Coals	Proximate analysis (wt. %)			Elemental composition (wt.%. daf)					Atomic ratio	
	M_{ad}	A_{ad}	V_{daf}	C	H	O	N	S	H/C	O/C
ZJ	1.8	21.3	17.5	91.4	3.1	4.2	0.2	1.0	0.41	0.03
HN	1.2	12.4	35.0	85.8	5.0	8.1	0.3	0.7	0.70	0.07
KL	1.2	13.2	33.5	78.5	5.6	13.7	1.2	0.3	0.85	0.13
SY	2.3	19.9	36.5	71.1	6.1	19.8	1.6	0.4	1.03	0.21

M: moisture; *A*: ash yield; *V*: volatile matter; ad: air dried basis. daf: dried ash free basis.

Table 3 Crystallite parameters of the studied coal samples

Coals		▲(°)		▼ (nm)			Coals		▲(°)		▼ (nm)		
		$2\theta_{002}$	$2\theta_{100}$	d_{002}	L_c	L_a			$2\theta_{002}$	$2\theta_{100}$	d_{002}	L_c	L_a
ZJ	raw coal	26.15	46.16	0.3498	1.9841	2.9922	KL	raw coal	25.58	45.56	0.3571	1.5786	2.9681
	25 ℃	26.17	44.64	0.3496	1.9848	2.9931		25 ℃	25.65	45.64	0.3562	1.5796	2.9684
	100 ℃	26.26	45.93	0.3485	1.9842	3.0073		100 ℃	25.58	46.20	0.3571	1.5786	2.9752
	200 ℃	26.21	45.09	0.3491	1.9842	2.9901		200 ℃	25.47	45.31	0.3585	1.5772	2.9689
	300 ℃	26.27	45.28	0.3483	1.9842	2.9850		300 ℃	25.54	46.55	0.3576	1.5781	2.9678
	400 ℃	26.26	44.38	0.3485	1.9837	2.9811		400 ℃	25.80	45.36	0.3543	1.5816	2.9683
	500 ℃	26.24	44.14	0.3487	1.9833	2.9782		500 ℃	25.73	45.36	0.3552	1.5806	2.9674
	600 ℃	26.35	44.61	0.3474	1.9868	2.9905		600 ℃	26.07	46.60	0.3509	1.5852	2.9685
	700 ℃	26.40	45.30	0.3468	1.9876	2.9925		700 ℃	26.03	46.20	0.3513	1.5847	2.9679
	800 ℃	26.54	45.02	0.3451	1.9897	2.9899		800 ℃	26.31	45.59	0.3479	1.5885	2.9682
	900 ℃	26.59	45.51	0.3444	1.9901	2.9773		900 ℃	26.29	45.70	0.3481	1.5882	2.9671
HN	Raw coal	25.66	45.72	0.3561	1.6786	2.9717	SY	raw coal	25.61	45.43	0.3567	1.3791	2.9613
	25 ℃	25.69	45.87	0.3557	1.6796	2.9598		25 ℃	25.61	44.61	0.3567	1.3791	2.9632
	100 ℃	25.65	45.66	0.3562	1.6786	2.9787		100 ℃	25.54	46.54	0.3576	1.3781	2.9681
	200 ℃	25.61	45.76	0.3567	1.6772	2.9591		200 ℃	25.54	45.31	0.3576	1.3781	2.9632
	300 ℃	25.72	45.01	0.3553	1.6781	2.9598		300 ℃	25.54	45.66	0.3576	1.3781	2.9779
	400 ℃	25.54	45.57	0.3576	1.6816	2.9528		400 ℃	25.47	45.30	0.3585	1.3772	2.9625
	500 ℃	25.63	46.72	0.3565	1.6806	2.9537		500 ℃	25.42	44.78	0.3592	1.3765	2.9667
	600 ℃	25.88	46.64	0.3532	1.6852	2.9587		600 ℃	25.64	46.01	0.3563	1.3794	2.9560
	700 ℃	25.89	45.87	0.3531	1.6847	2.9504		700 ℃	25.76	45.71	0.3548	1.3812	2.9615
	800 ℃	26.17	45.60	0.3496	1.6885	2.9542		800 ℃	25.88	43.53	0.3532	1.3826	2.9581
	900 ℃	26.19	45.66	0.3493	1.6882	2.9393		900 ℃	25.92	44.67	0.3527	1.3832	2.9590

▲: Diffraction angle; ▼: Structural parameters.

Table 4 Thermal characteristics parameters of thermogravimetric analysis of the studied coals

Coals	$W_{100\text{-}750°C}$ (%)	$W_{100\text{-}300°C}$ (%)	$W_{300\text{-}500°C}$ (%)	$W_{500\text{-}600°C}$ (%)	$W_{600\text{-}750°C}$ (%)	T*i* (°C)	T_{DTGmax} (°C)
ZJ	89.4	3.1	1.8	57.5	25.2	450	600
HN	85.8	1.7	3.7	41.0	39.1	414	528
KL	89.0	3.4	40.1	36.8	5.1	387	517
SY	82.3	3.5	64.8	12.5	0.6	251	454

W: Mass loss between different temperature intervals.

T*i*: Temperature of initial thermal decomposition.

T_{DTGmax}: Temperature of maximum rate of mass loss.

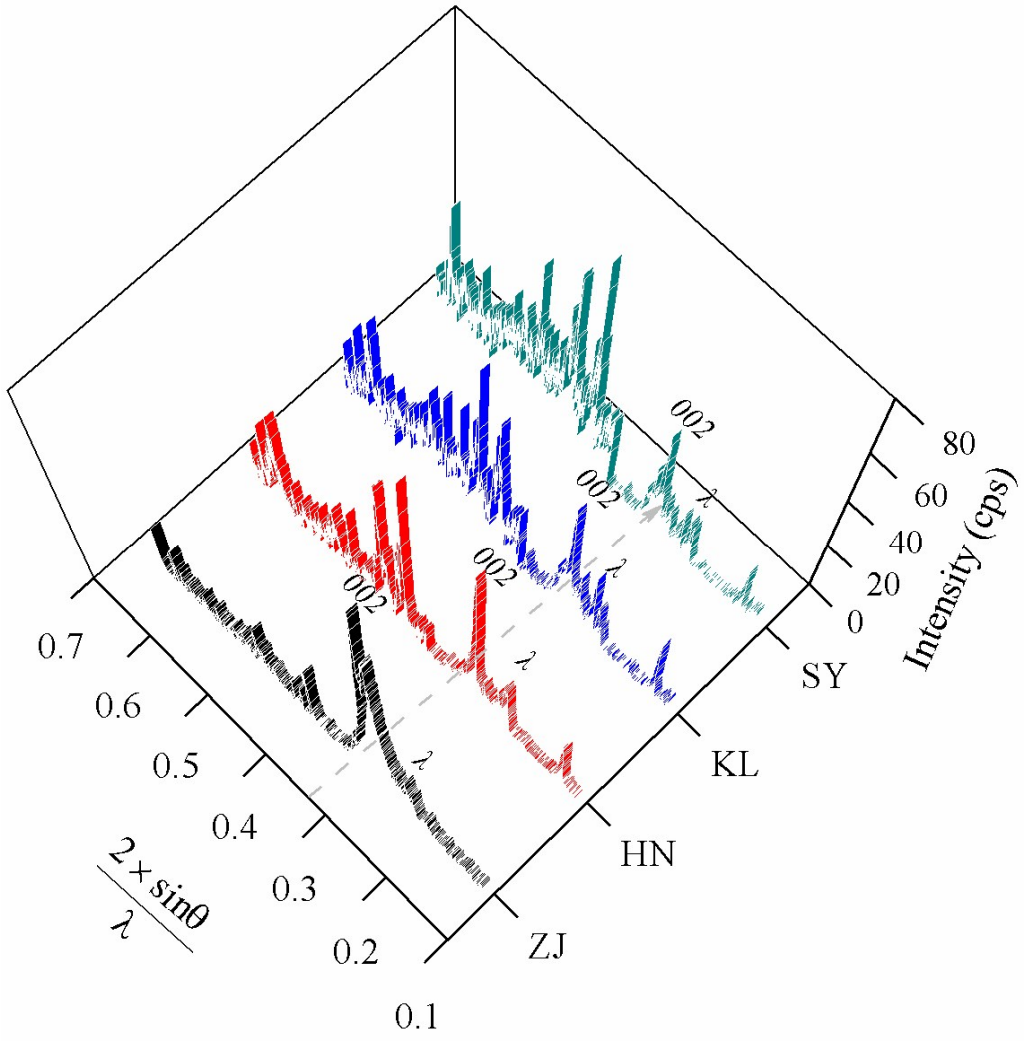

The XRD profiles of raw coal